5-2020

Analysis of Road Salt Loading and Transport in the Wachusett Reservoir Watershed

Joshua Soper
University of Massachusetts Amherst

Analysis of Road Salt Loading and Transport in the Wachusett Reservoir Watershed

A Masters Project Presented

by

Joshua Soper

Submitted to the Graduate School of the University of Massachusetts Amherst in partial fulfillment of the requirements for the degree of

MASTER OF SCIENCE

in

Civil Engineering

May 2020

Department of Civil and Environmental Engineering

University of Massachusetts

Amherst, MA 01003

Analysis of Road Salt Loading and Transport in the Wachusett Reservoir Watershed

A Masters Project Presented

by

Joshua Soper

Approved as to style and content by:

DocuSigned by:
John E. Tobiason
301851AAB6FD48F...
Dr. John E. Tobiason
Committee Chairperson

DocuSigned by:
Emily Kumpel
E4F23C5B4E8A4D1...
Dr. Emily Kumpel
Committee Member

DocuSigned by:
Colin Gleason
86282A4A8CB34B6...
Dr. Colin Gleason
Committee Member

DocuSigned by:
7A038FBD5187469...
Dr. Christian Guzman
Committee Member

DocuSigned by:
01F608E2CB7F4FD...
Caitlyn Butler
Civil and Environmental Engineering Department

Acknowledgments

This research was supported by the Department of Conservation and Recreation (DCR) and the Massachusetts Water Resources Authority (MWRA). I would like to thank all of the DCR and MWRA employees, namely Larry Pistrang, Dan Crocker, and Jamie Carr, for their continued support of and involvement in our reservoir system research. Thank you to my advisor, Dr. John Tobiason, for his commitment to my graduate studies. His flexibility has allowed me to pursue my personal research interests, both within and beyond the context of the DCR projects. His experience and driven mentorship did not go unnoticed during my 6 years spent at UMass. I would also like to thank the members of my committee, professors Emily Kumpel, Colin Gleason, and Christian Guzman, for their contributions and unique insights. I truly appreciate the willingness of my committee members to provide support and answer questions at a moment's notice. A special thank you to Colin Gleason, whose flip of a coin persuaded me to pursue graduate work in the first place. And thank you to my research partner, Nelson Da Luz, for serving as a guiding voice in my studies.

Additionally, I would like to thank Dr. Lily Jeznach for her exceptional modeling documentation and continued involvement with the project. Thank you, Don Park and Chinedum Eluwa, for your technical expertise and insights into the minds of the machines that produce efficient work. A thank you to Merritt Harlan, Xuyen Mai, Sarah Pfeifle, and all other EWRE students for being excellent listeners and being willing to entertain my routine office visits. And to the current and former EWRE graduate students, family, friends, and my partner, thank you for your support that has made my life-long Amherst education worth it.

Abstract

Chloride exports from the widespread application of road salt serve as a primary contribution to water body salinity in cold climate regions. The detrimental effects of road salt pollution on water quality include an apparent relationship between chloride and water corrosivity. This study utilizes regression based chloride load estimation to support mass balances and analyze transport flow-paths to the Wachusett Reservoir from its predominantly rural watershed. Results from hydrograph and load separation techniques show that average loading and discharge from baseflow contributed approximately 74% and 65% of the total loading and discharge, respectively. The baseflow dominated tributary chloride loading is not only a result of predominantly baseflow sustained discharge, but is also attributed to enhanced groundwater chloride concentrations that result from road salt transport favoring sub-surface infiltration. However, a long-term trend analysis suggests a slight shift towards an increased fraction for chloride loading via overland flow, perhaps as a result of late 20th century land development. Load estimation with LOADEST was generally insensitive to a variety of hydrograph separation methods, yet yearly estimates from LOADEST offered similar accuracy to those from simple linear interpolation. A chloride mass balance performed for 2000-2019 revealed that reservoir and watershed export only recently reached a level similar to inputs from road salt over the 20-year period of study. The decadal response of the reservoir system reflects the slow-moving nature of the baseflow dominated chloride loading and implies that decreased road salt application will not likely be reflected in near-term outflowing reservoir water quality. It is recommended that current and future corrosion control practices for drinking water treatment should consider chloride persistence in the reservoir.

Table of Contents

List of Figures

List of Tables

1. Introduction

Road salt application for roadway deicing purposes is a standard practice in cold climate regions. Widespread use in the U.S. originated during the 1940s (Kelly, T. D. et al., 2010), with rock salt (NaCl) the most commonly used deicer due to its low cost, effective dispersion properties, and ease of storage (Ramakrishna and Viraraghavan, 2005). Road salt induced freshwater salinization was first recognized in the late 1960s and ear1y 1970s (Hutchinson and Olson, 1967; Judd, J. H., 1970), followed by observations of road salt contamination in rivers (Godwin et al., 2003; Dailey et al., 2014), streams (Kelly, V. R. et al., 2007; Trowbridge et al., 2010; Moore et al., 2019), lakes (Novotny et al., 2008; Likens and Buso, 2010), and groundwaters (Huling and Hollocher, 1972; Howard and Haynes, 1993; Meriano et al., 2009; Perera et al., 2013). Other potential sources of chloride include the natural weathering of rocks, atmospheric deposition, agricultural fertilizers, chemical and food production, seawater intrusion, water softening, and wastewater and septic system effluent (Panno et al., 2006; Novotny et al., 2009). However, chloride inputs are often dominated by road salting in regions where they are applied (Moore et al., 2019).

Concerns over surface and sub-surface water quality impairment due to road salting practices are ever-mounting. In lakes and reservoirs, elevated chloride concentrations (the preferred environmental tracer due to its highly conservative nature) from deicers have been shown to alter density gradients and mixing dynamics, such that periods of complete mixing in lakes are either delayed or exhibit perennial meromixis (i.e. permanent stratification) (Bubeck and Burton, 1989; Sibert et al., 2015; Wyman and Koretsky, 2018) . As an indirect consequence of meromixis, water bodies may exhibit severe states of hypolimnetic anoxia (Judd, K. E. et al., 2005), enhanced eutrophication (Novotny and Stefan, 2012; Koretsky et al., 2012), and trophic structure

disruption (Hintz et al., 2017). At smaller scales, vernal pool breeding amphibians have exhibited a heightened sensitivity to dissolved chloride (Karraker et al., 2008; Collins and Russell, 2009) whereas native plant communities may become displaced by invasive, salt tolerant vegetation (Wilcox, 1986; Richburg et al., 2001). The aforementioned water quality concerns were reported for chloride concentrations typically in excess of the U.S. EPA chronic (four-day average once every three years) aquatic toxicity criteria of 230 mg/L or near the acute (one-hour average once every three years) toxicity of 860 mg/L. The U.S. EPA dissolved chloride secondary standard for drinking water taste is 250 mg/L.

Studies have shown that increasing concentrations of lead and copper in drinking water systems, as a result from corroded distribution infrastructure, are positively correlated with values of the chloride to sulfate mass ratio (CSMR) and Larson Ratio (Lytle et al., 2005; Edwards and Triantafyllidou, 2007; Ng and Lin, 2016; Stets et al., 2018). Where sulfate-lead interactions have been shown to form beneficial precipitates, chloride-lead reactions may introduce harmful soluble complexes into drinking water systems (Nguyen et al., 2011). In particular, a drastic change in the CSMR is frequently cited as a potential indicator for the enhanced water corrosivity observed during the Flint, Michigan water crisis (Masten et al., 2016; Pieper et al., 2017; Pieper et al., 2018). Larger surface waters, often benefiting from diluted pollutant levels, are more likely to have lower chloride concentrations (<100 mg/L) cited to potentially impact water corrosivity. Given the inability of most conventional water treatment practices to remove dissolved chloride, alternative chloride control measures are of importance for management authorities attempting to mitigate the effects of road salt pollution.

Rock salts are conservatively transported to receiving waters via quick (hours to days) overland flow as runoff or via slow (months to decades) sub-surface groundwater as baseflow

(Ostendorf and Kilbridge, 2011; Sanford and Pope, 2013; Starn and Belitz, 2018). Rates of catchment chloride export may be estimated using comprehensive mass balance approaches and are useful for determining site-specific groundwater storage tendencies by comparison to road salt application rates (Huling and Hollocher, 1972; Howard and Haynes, 1993; Perera et al., 2013). Riverine chloride loads are calculated as the product of volumetric discharge and chloride concentration integrated over a specified time period. Tributary loading separated by flow-path (i.e. loading disaggregated into components of baseflow and runoff) is more difficult to assess and requires timeseries of discharge and concentration representative of baseflow conditions. Baseflow data may be derived from dry-period assumptions (Howard and Haynes, 1993), directly measured with groundwater sampling (Meriano et al., 2009), or estimated with regression based modeling approaches (Cohn et al., 1989; Cohn et al., 1992), the latter of the three a desirable option when conditional baseflow assumptions are not appropriate year-round and reliable groundwater data are not available.

The United States Geologic Survey (USGS) program LOADEST (Runkel et al., 2004) is one of the most commonly employed statistically based water constituent load estimation methods, and relates log transformed load to functions of streamflow and decimal time. Given that water quality constituents are rarely measured with high frequency (typically occurring at weekly, bi-monthly, or even longer timesteps), regression models may offer an accurate approach to estimate constituent loading between known measurements (Pellerin et al., 2014). Constituents assessed using LOADEST models include nitrogen, (Schilling and Zhang, 2004; Jha et al., 2007), phosphorus (Chen et al., 2015), suspended solids (Duan et al., 2013), and TDS (Shope and Angeroth, 2015). Moreover, separate baseflow loading regression models are considered in Schilling and Zhang (2004) , Wang et al. (2015) , and He et al. (2020).

The goal of the current study is to quantify the impacts of road salting practices on chloride loading in a predominantly rural watershed for a drinking water supply reservoir (the Wachusett Reservoir). The study site benefits from a rich history of research (Ahlfeld et al., 2003; Hagemann and Park, 2014; Jeznach et al., 2016) and long-term data availability. The objectives of this study are threefold: (1) determine the primary chloride transport pathways from source to surface water; (2) perform a reservoir system chloride mass balance over a decadal period of study (2000 – 2019); (3) evaluate the performance and sensitivities of the regression models used. Few studies have assessed the impacts of road salting practices on drinking water reservoir systems (Nimiroski and Waldron, 2002; Ostendorf, 2013), and none have done so over a long-term study period. Furthermore, this study introduces a novel application of LOADEST regression modeling applied to road salt induced chloride loading.

2. Methods

2.1. Site description

2.1.1. MWRA system

The Wachusett Reservoir is located in Central Massachusetts and serves as a key component for the delivery of potable water to the greater metropolitan area of Boston. The two primary agencies that monitor and manage the reservoir are the Massachusetts Department of Conservation and Recreation (DCR) Division of Water Supply Protection and the Massachusetts Water Resources Authority (MWRA). Greater Boston's potable water quality, noted by its status as one of a handful of large unfiltered surface water systems in the U.S., is held in high regard; however, issues pertaining to its water corrosivity remain a concern for Massachusetts water authorities. In 1996, the addition of sodium carbonate and carbon dioxide in drinking water

treatment processes for corrosion control helped decrease historically high lead levels below the U.S. EPA Action Level of 15 ppb (Karalekas Jr et al., 1983). The management authorities continue to monitor water corrosivity and are particularly concerned with rising chloride concentrations in withdrawals from the Wachusett Reservoir via the Cosgrove Intake (Fig. 1).

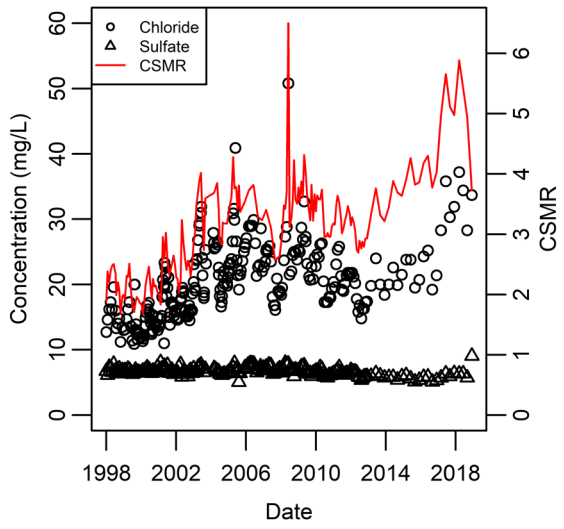

Fig. 1. Historic chloride, sulfate, and chloride to sulfate mass ratio (CSMR) observed at the primary Wachusett Reservoir withdrawal (Cosgrove Intake).

2.1.2. Study site

The Wachusett Reservoir is a dimictic surface water located approximately 10 kilometers northeast of Worcester, MA. The 16.3 km^2 water body receives an average annual precipitation and snowfall of 1,260 mm and 1,960 mm, respectively, over a predominantly rural (87%) 287 km^2 watershed area. The Wachusett Reservoir is fed by periodic transfers from the Quabbin Reservoir, located approximately 50 kilometers to the west, and ten tributaries monitored by the DCR, located to the north, west, and south of the reservoir (Fig. 2). The watershed delineation was performed and provided by the DCR. Additionally, a 26 km^2 runoff area borders the reservoir shoreline, providing direct inflow without entering a monitored tributary. Select

watershed characteristics by tributary are summarized in Table 1, with mean tributary chloride concentrations showing a direct correlation to impervious surface and paved surface density (Fig. 3). Land use within the watershed (derived from the MassGIS Land Use – 2005 data layer: https://docs.digital.mass.gov/dataset/massgis-data-layers) is primarily forest/forested wetland (73%), very-low to medium density residential (10%), and cropland (3%). Total impervious surface coverage accounts for 5% of the watershed area, of which 14% is attributed to transportation. Land development within the watershed has continued to increase since the 1970s (Table 2), marked by increases in residential density and the completion of US Route 190. During the same period, the MWRA and DCR have continued to purchase land within the watershed. Anomalously high land development fractions in 2016 were calculated with a separate dataset that used differing land use codes from prior years.

Table 1. Reservoir watershed hydrologic characteristics and chloride trends by tributary. Coefficient of determination (R^2) reflect positive linear regressions between observed daily chloride concentrations and date (days) for 2000-2019, all of which are statistically significant with 99% confidence.

Reservoir Input (abbr.)	Area (km^2)	2000-2019 Mean Discharge (m^3/s)	Percent Impervious Surface (%)	1990 Mean $[Cl^-]$[1](mg/L)	2019 Mean $[Cl^-]$[1] (mg/L)	R^2
Direct Runoff (DR)	26.5	0.55	5.9	-	-	-
French Brook (FB)	5.5	0.11	6.3	14	74	0.27
Gates Brook (GB)	5.2	0.12	20.2	87	297	0.33
Malagasco Brook (MgB)	2.3	0.05	9.1	34	129	0.18
Malden Brook (MaB)	6.6	0.14	7.4	25	88	0.27
Muddy Brook (MuB)	1.9	0.04	9.0	22	80	0.17
Quabbin Transfer (QT)	-	5.61	-	4.2	8.6	
[2]*Quinapoxet River (QR)*	125.5	2.11	5.8	-	59	0.03
Stillwater River (SR)	78.5	1.63	3.9	7	35	0.13
Trout Brook (TB)	17.5	0.37	2.5	2	12	0.04
Waushacum Brook (WB)	16.1	0.34	9.3	32	98	0.24
West Boylston Brook (WBB)	0.9	0.02	14.1	79	327	0.20
Total	**287**	**5.47**	**15.8 (km^2)**	**34**	**120**	**-**

[1]Approximated from measurements of specific conductivity
[2]Period of record begins in 2000

Table 2. Developed land use coverage as a fraction of total sub-basin area.

Tributary	1971	1985	1999	2016
QR	0.10	0.13	0.16	0.42
SR	0.05	0.10	0.13	0.39
WB	0.14	0.22	0.25	0.45
MaB	0.22	0.29	0.31	0.49
FB	0.18	0.19	0.24	0.52
GB	0.52	0.60	0.62	0.78
MgB	0.16	0.24	0.26	0.62
Mub	0.22	0.22	0.23	0.41
WBB	0.43	0.51	0.56	0.77
Median	**0.18**	**0.22**	**0.25**	**0.49**

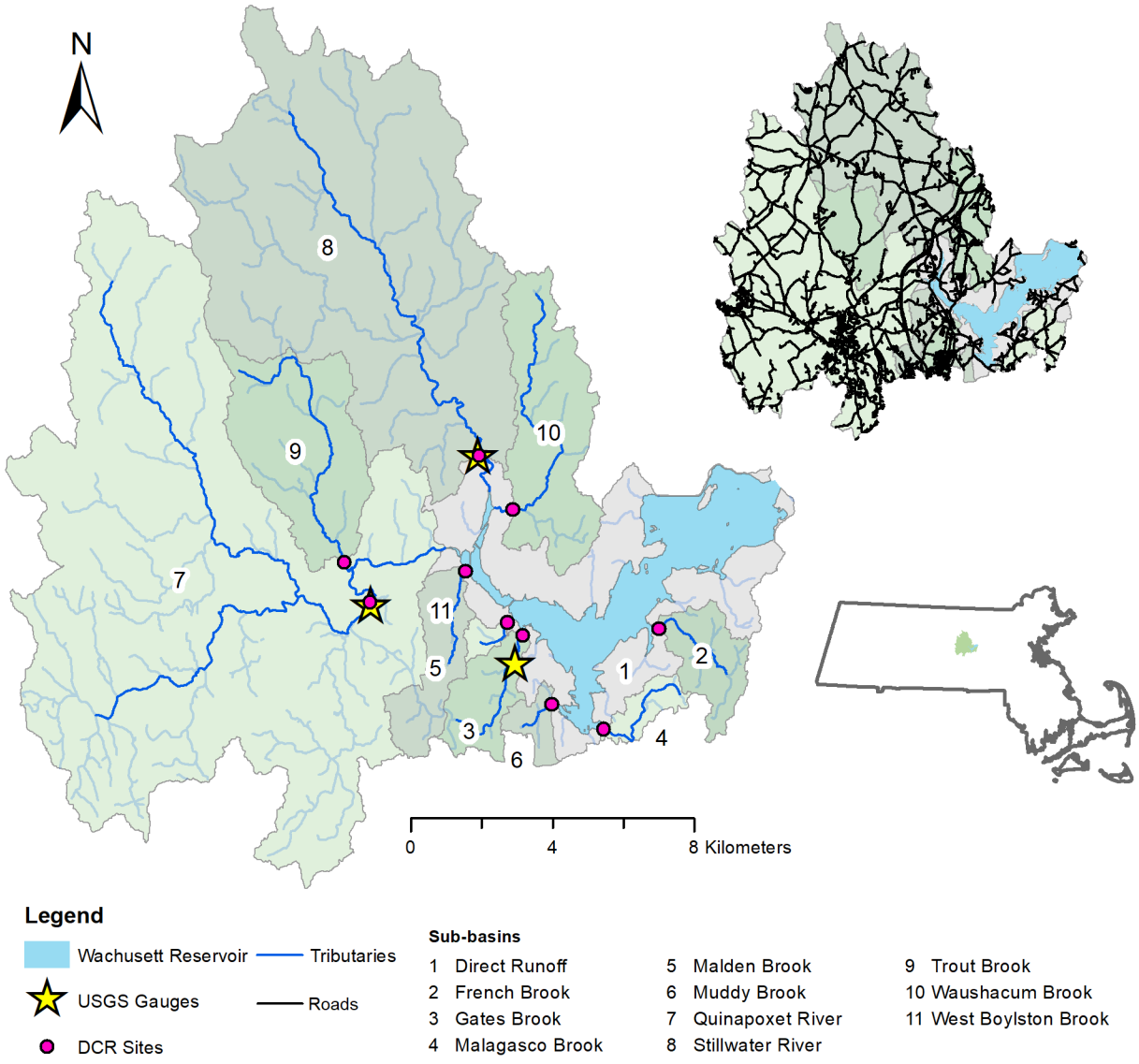

Fig. 2. Wachusett Reservoir watershed study area and roadway network.

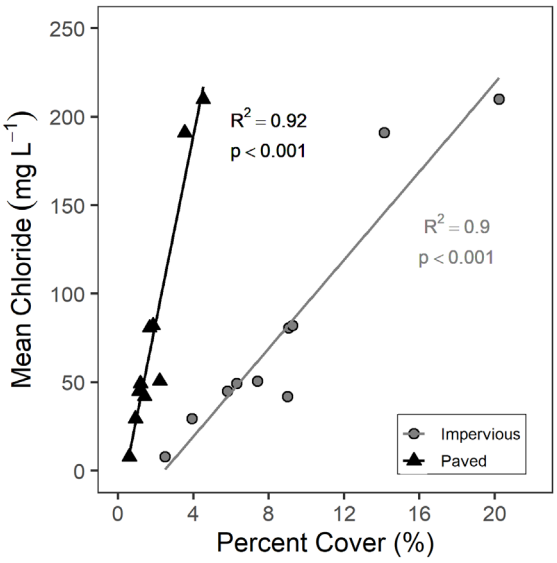

Fig. 3. Linear regression between mean tributary chloride concentration (2000-2019) and its corresponding percentage of watershed area as impervious and paved surface.

2.2. LOADEST model development

LOADEST regression models were used to estimate daily tributary chloride loading in the absence of daily concentration data. The regression formulas relate log-transformed load (L) to functions of centered streamflow (Q) and/or centered decimal time (t). The explanatory variables are centered to avoid multicollinearity during regression (Cohn et al., 1992). LOADEST model coefficients are calibrated to observed loads (computed with measurements of discharge and concentration) using Adjusted Maximum Likelihood Estimation (AMLE), an estimation approach that accounts for censored data subject to a normality of residuals assumption (Runkel et al., 2004). 'Total' and 'baseflow' regression models were developed for each of the ten tributaries using the full 20-year period of study. The R package 'rloadest' (https://github.com/USGS-R/rloadest) was used as a substitute for the original LOADEST program. The following sections detail the methods used for both total and baseflow model construction.

2.2.1. Hydrograph separation

Total tributary flow timeseries were obtained either from USGS gauging stations or calculated based on the Stillwater River daily flow (Tobiason et al., 2002). The Quinapoxet River and Stillwater River daily flow observations were provided by USGS gauges for the entire study period. Gauged flow for the Gates Brook was collected starting in October of 2011. Daily flow estimates (at timestep *t*) for the remaining seven minor tributaries and for Gates Brook (prior to 2012) were calculated based on the daily watershed yield of the Stillwater River and sub-basin area of interest (Eq. 1)

$$\mathrm{Q_{Trib_t}} = \mathrm{Q_{Stillwater_t}}\left(\frac{\mathrm{Area_{Trib}}}{\mathrm{Area_{Stillwater}}}\right) \quad \text{(Eq. 1)}$$

Several methods for separating tributary hydrographs into components of baseflow and runoff were considered and include the USGS HYSEP program from Sloto and Crouse (1996), the PART program from Rutledge (1998) and digital separation filters from Lyne and Hollick (1979) and Eckhardt (2005).

The Lyne and Hollick (L&H) one-parameter digital recursive filter is derived from signal processing theory and attributes the low-frequency component of streamflow to baseflow. The L&H filter was employed in this study using the R package 'EcoHydRology' (Fuka et al., 2014) with a filter parameter of 0.925 as proposed by Nathan and McMahon (1990) and several filter passes (one, two, and three) that govern the degree of smoothing. The two parameter Eckhardt filter assumes that aquifer discharge is linearly proportional to its storage and introduces the concept of a maximum achievable baseflow index (BFI), where BFI is the ratio of baseflow volume to total discharge volume for a specified long-term time period. The inclusion of a maximum BFI, assumed equal to 0.8 for this study as per Eckhardt (2005), allows for the

attribution of a non-negligible low-frequency component of streamflow to runoff, as noted by Spongberg (2000). The Eckhardt baseflow separation was calculated using the R package 'FlowScreen' (Dierauer and Whitfield, 2017).

The HYSEP and PART programs rely upon a linear interpolation between a subset of discharge measurements that are assumed equal to baseflow. The HYSEP program includes three separation algorithms (fixed-interval, sliding-interval, and local-minimum) to systematically differentiate between baseflow and runoff. Details of each method are provided in Sloto and Crouse (1996) as originally developed by Pettyjohn and Henning (1979). The PART program uses an antecedent recession requirement to develop the initial subset of discharge data attributed to baseflow. Streamflow separation is a function of catchment area in both the HYSEP and PART programs and were calculated using the USGS R package 'DVStats' (https://github.com/USGS-R/DVstats).

The BFI, calculated for the period 10/2011 – 12/2019, for each of the eight different methods (Table 3) reveal the range of potential baseflow timeseries for load estimation. The 2011-2019 timeframe represents the period of record for which all three USGS gauges were in simultaneous operation. The numbers following the "L&H" designation refer to the number of filter passes. The letters following the "HYSEP" designation refer to the program's baseflow separation method; local-minimum (L), fixed-interval (F), and sliding-interval (S). Ultimately, the HYSEP-L (local-minimum) method was chosen for this study given its application in New England based studies (Hodgkins and Dudley, 2011) and that the resultant mean BFI (0.68) most closely represents an average of the available methods (0.685). The local-minimum method utilizes a linear interpolation between the lowest-flows of a hydrograph within a set of calculated intervals that depend on catchment area. Model sensitivities to the varying baseflow separation methods

were ultimately explored given the inherent importance of flow on loading estimates (Zhu et al., 2019).

Table 3. Baseflow index by tributary and separation method for 10/2011 – 12/2019.

Tributary	Eckhardt	HYSEP-F	HYSEP-L	HYSEP-S	L&H1	L&H2	L&H3	PART
GB	0.756	0.755	0.699	0.753	0.719	0.604	0.54	0.761
QR	0.775	0.719	0.682	0.723	0.725	0.592	0.514	0.782
SR	0.755	0.752	0.659	0.759	0.682	0.545	0.471	0.719
Mean	0.762	0.742	0.680	0.745	0.709	0.580	0.508	0.754

2.2.2. Concentration separation

Weekly to bi-monthly grab-sample based measurements (collected by the DCR) of specific conductivity (µS/cm) were used to develop separate timeseries for total and baseflow chloride concentrations. Specific conductivity (SC) was converted to chloride ([Cl^-] in mg/L) using a linear regression (Eq. 2; $R^2 = 0.996$) developed for 2018 data. Total chloride concentration is defined as the chloride level calculated from measured SC. It was assumed that baseflow chloride concentration equaled total chloride for days when baseflow exceeded 90% or more of the total streamflow (Schilling and Zhang, 2004; Wang et al., 2015), a threshold deemed appropriate for returning a large enough baseflow chloride sample size. Two sample outliers (defined as an observation that deviated one order of magnitude from the sample mean) from the Muddy Brook chloride timeseries and one sample outlier from both the Malden Brook and West Boylston Brook timeseries were removed from the regression calibration dataset.

$$[\mathrm{Cl}^-](\mathrm{mg\,L^{-1}}) = -11.16 + 0.267\mathrm{SC}(\mu\mathrm{S\,cm^{-1}}) \quad \text{(Eq. 2)}$$

2.2.3. Model selection

The optimum regression equation from a suite of nine pre-defined formulas was automatically selected for each tributary based on the minimum calculated Akaike Information Criterion (AIC) statistic (Runkel et al., 2004). Schwarz Posterior Probability Criterion (SPPC) statistics were also calculated during the model selection process, but were not factored into the optimum model selection. The performance of each model was assessed by its coefficient of determination (R^2), Nash-Sutcliffe Efficiency (NSE) (Nash and Sutcliffe, 1970), load bias percentage (Bp), and an analysis of model residuals. The optimum regression formulas as determined by LOADEST are summarized in Table 4. All tributary chloride loads were estimated using model number 9, with the exception of the total (model 8) and baseflow (model 7) Stillwater River regressions.

Table 4. Summary of LOADEST regression equations

Model	Equation
7	$\ln(L) = a_0 + a_1\ln(Q) + a_2\sin(2\pi t) + a_3\cos(2\pi t) + a_4 t$
8	$\ln(L) = a_0 + a_1\ln(Q) + a_2\ln(Q^2) + a_3\sin(2\pi t) + a_4\cos(2\pi t) + a_5 t$
9	$\ln(L) = a_0 + a_1\ln(Q) + a_2\ln(Q^2) + a_3\sin(2\pi t) + a_4\cos(2\pi t) + a_5 t + a_6 t^2$

2.3. Mass balance

Sub-basin scale chloride mass budgets were developed by balancing inputs from road salts with exports from tributary loading. NaCl inputs for each sub-basin were estimated by multiplying specific application rates (expressed as ton/lane-mi per year) for the Massachusetts Department of Transportation (MassDOT), local cities/towns, and private maintenance (parking lots) by their respective lane-mile coverage. Geographical Information Systems (GIS) software coupled with publicly available MassGIS data (https://docs.digital.mass.gov/dataset/massgis-data-layers) were used for all spatial analysis in this study unless noted otherwise. The MassDOT

Roads layer was used to estimate lane-mile coverage per sub-basin and roadway jurisdiction (MassDOT or city/town). Estimates of privately maintained paved surfaces were developed by taking the intersection of impervious surface coverage with commercial or multi-family residential land uses and removing all rooftop surface areas. The resultant area was converted to lane-miles assuming a uniform 3.7 meter lane-width. An average road salt application rate of 42.3 ton/lane-mi for DOT maintained roads was used as per the 2017 Environmental Status Planning Report for District 3 (MassDOT, 2017). Yearly mass inputs of road salt into the watershed by town were provided by the DCR and equally allocated into each intersecting sub-basin on a percentage lane-mile basis. Roadway coverage outside cities/towns that reported data received an application rate of 31.6 ton/lane-mi, equal to the average city/town rate. Privately maintained paved surfaces also received an application rate equal to the city/town rate of 31.6 ton/lane-mi.

Other sources of chloride considered in this study include septic system effluent and wet deposition. Chloride inputs from human excretion and domestic waste products are estimated as 12.4 kg per person per year and four people per septic parcel (Kelly et al., 2007). Historic septic system data (temporal and spatial) by parcel were provided by the DCR. Wet deposition loads were calculated as the product of daily precipitation reported by the National Oceanic and Atmospheric Administration (NOAA) at Worcester Airport and atmospheric chloride concentration, measured at the Quabbin Reservoir and reported by the National Atmospheric Deposition Program (NADP). There is no wastewater discharged from treatment facilities within the reservoir watershed.

3. Results / Discussion

3.1. Flow-path transport

The annual baseflow load index (BLI), defined as the yearly fraction of total load attributed to baseflow, by tributary for water years 2001 through 2019 is shown in Fig. 4a. Mean (0.74) and median (0.73) BLIs were computed for nine of the ten watershed tributaries (Trout Brook was excluded due to poor model performance). The largest mean BLIs were attributed to the Stillwater River (0.84) and Malagasco Brook (0.9) whereas the lowest mean BLI was attributed to the Waushacum Brook (0.59).

A baseflow chloride index (BCI), in the manner of Schilling and Zhang's (2004) baseflow enrichment ratio (BER), is introduced in this study. The BCI formula (Eq. 3) represents the ratio of the BLI to the BFI for any given year. It is effectively a baseflow concentration metric normalized to the total observed tributary concentration. The annual BCI distributions by tributary (Fig. 4b) range from 0.99 to 1.56, with a mean value of 1.14. The largest BCIs are again associated with the Stillwater River ($\overline{\text{BCI}}$ = 1.24) and Malagasco Brook ($\overline{\text{BCI}}$ = 1.30).

$$\text{BCI} = \frac{\text{BLI}}{\text{BFI}} \qquad \text{(Eq. 3)}$$

The high fractions of loading attributed to baseflow, and minor contributions from runoff, were present in all reservoir tributaries. Results from previous studies in urban watersheds are significantly lower, with baseflow loading contributions ranging from 40% – 48% in Meriano et al. (2009) and Perera et al. (2013) up to 61% in Ostendorf (Ostendorf, 2013). Ostendorf accounts for interflow chloride loading (17% of the total) which is the mass flux attributed to the transition between high-discharge stormflow and low-discharge baseflow. Using the local-minimum HYSEP methodology, the interflow periods accounted for in Ostendorf (2013) would likely be

considered as runoff, however this claim is only speculation. Conversely, studies in more rural watersheds have assumed a baseflow load index of 0.9 (Kelly et al., 2007; Shaw et al., 2012). Ultimately, BLIs are governed by baseflow hydrology and difficult to use as a tool to properly evaluate road salt transport characteristics.

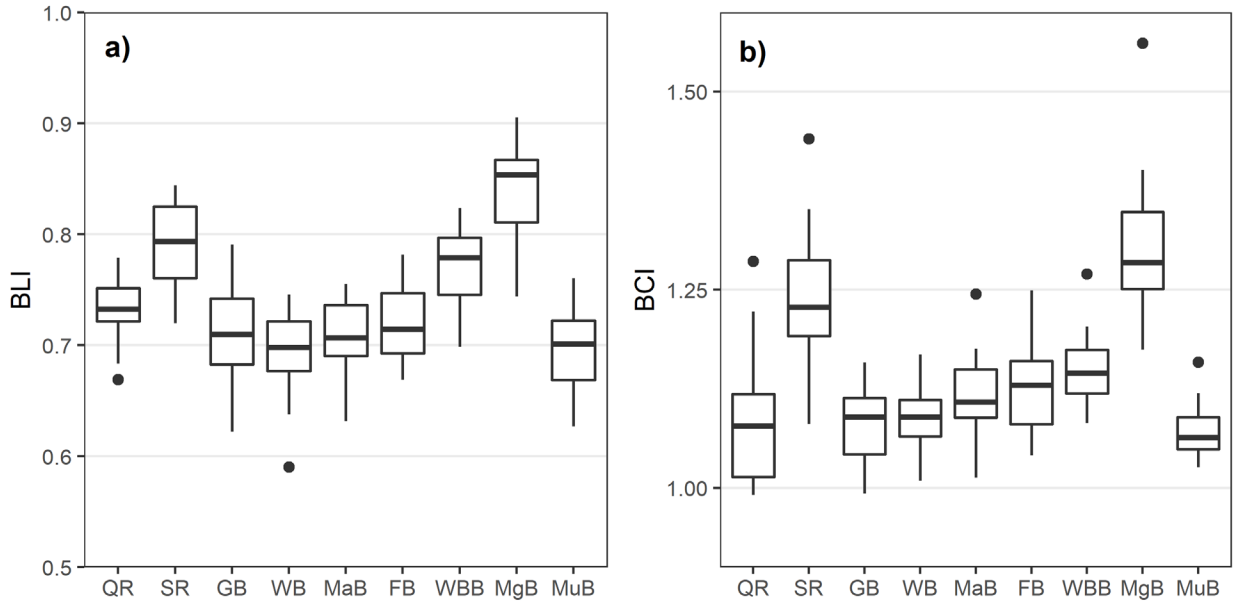

Fig. 4. Yearly fraction of total chloride load due to baseflow (a) and corresponding baseflow chloride index (b) by tributary for water years 2001 through 2019.

The BCI (Fig. 4b.) offers a unique means for identifying the favored flow-paths, or drainage tendencies, that road salts take to surface waters. The mean tributary BCI of 1.14 suggests that road salts infiltrate into groundwater sources at a higher rate than runoff as overland flow. This phenomenon seemingly reflects the rural nature of the watershed. Immediate transport to receiving waters via overland flow and drainage infrastructure becomes less likely with decreased impervious coverage density. Furthermore, the watershed transportation network is dominated by low traffic roads that may be devoid of drainage infrastructure. Instead of travelling through culverts and stormwater collection systems, the road salts applied on low-

traffic roads are suspected to drain directly into the adjacent pervious (predominantly forested) surfaces.

It was expected that correlations could be drawn between a catchment's drainage tendencies and its impervious surface density (ISD) using the BCI. While the Gates Brook (ISD = 20%; $\overline{BCI}$ = 1.08) and West Boylston Brook (ISD = 14%; $\overline{BCI}$ = 1.15) contributed lower proportions of chloride load through baseflow when compared to the more rural catchment feeding the Stillwater River (ISD = 3.9%; $\overline{BCI}$ = 1.30), BCI results from the remaining catchments ranged from 1.07 to 1.24 and did not seem to adhere to any relationship with ISD (ranging from ~6% – 9%). Given the rural nature of the watershed, a sub-basin scale assessment of drainage infrastructure would likely be needed to further distinguish sub-basin BCI trends. It is important to note that baseflow chloride signatures may not represent the total amount of infiltrated road salts given that a proportion of chloride in sub-surface storage may seep into fractured bedrock (Vitale et al., 2017). Underlying bedrock characteristics were not assessed in this study but are expected to vary by sub-basin. The lack of a correlation to ISD may also be attributed to LOADEST model or streamflow model error. Smaller catchment (<10 km^2) hydrographs used in this study are derived from relatively dispersed runoff events in the Stillwater River (~ 80 km^2). When combined with observed concentration data, errors in the simple hydrologic modeling approach could propagate into the baseflow separation and regression techniques employed in this study.

The relationships between total flow, total load, and mean concentration aggregated by all reservoir tributaries are shown in Fig. 5. Mean concentration and total flow were inversely correlated, exhibiting local maxima and minima, respectively, near the beginning and end of the

study period. The 2005 – 2012 period were high-flow water years that translated to generally lower chloride concentrations.

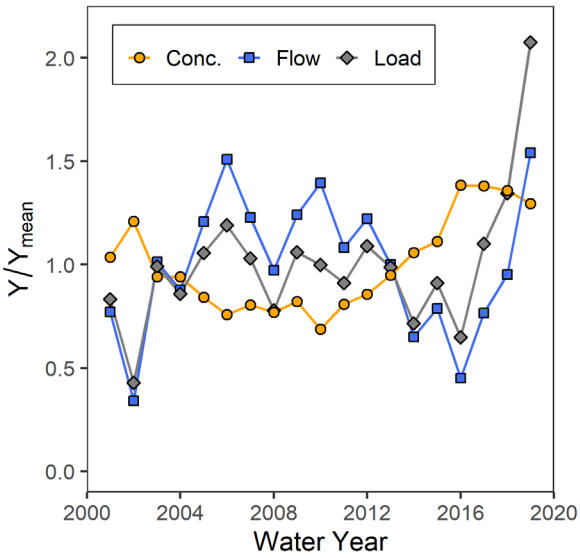

Fig. 5. Normalized yearly observations of mean chloride concentration, total flow, and total chloride load aggregated over all reservoir tributaries.

The BCI variation by water year and tributary are provided in Fig. 6. A Mann-Kendall (MK) monotonic trend test for the mean tributary BCI from water years 2001 through 2019 suggests a statistically significant ($p < 0.05$) decreasing trend (MK correlation coefficient, $\tau = -0.37$) in mean BCI over time. Three of the nine modeled tributaries, the Quinapoxet River ($\tau = -0.64$; $p < 0.001$), Gates Brook ($\tau = -0.56$; $p < 0.01$), and French Brook ($\tau = -0.42$; $p < 0.05$), exhibited statistically significant decreasing trends during the study period. The remaining tributaries either exhibited statistically insignificant ($p < 0.07$), yet apparent decreasing trends (range in τ from -0.31 to -0.33), or in the case of the Waushacum, West Boylston, and Malagasco brooks, no clear trend at all ($-0.2 < \tau < 0$; $p > 0.3$). MK trend tests were chosen in lieu of a large sample size ($n = 19$).

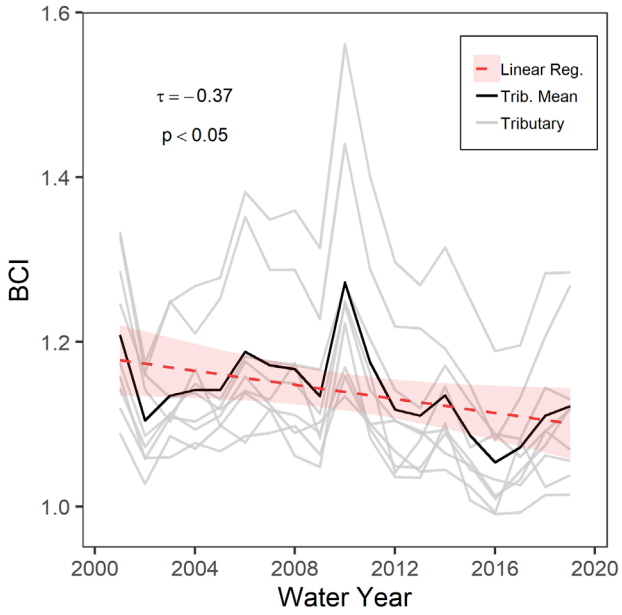

Fig. 6. Baseflow chloride index versus water year per tributary. Linear regression and 95% confidence interval (red area) illustrate a negative trend of the tributary average.

Given that the majority of chloride mass is gradually delivered through slow-moving baseflow, BCI values in large part reflect the impact of road salting practices from prior years and decades. Therefore, the apparent decreasing mean BCI trend during this study period is possibly attributed to increases in watershed land development observed during the late 20th century (Table 2). As eluded to earlier, the steadily increasing impervious surface coverage offers new direct-transport mechanisms for applied road salts to receiving waters. The year to year variation in BCI, however, are largely a function of groundwater hydrologic dynamics, and somewhat counterintuitively, share a positive correlation with precipitation and streamflow discharge. A spike in 2010 water year BCI may be explained by a preceding series of heavy precipitation years that culminated in groundwater saturation, such that any additional precipitation was ultimately re-routed as overland flow. As fractions of heavy precipitation induced runoff increase, reduced BFIs drive relative sub-surface chloride concentrations up. Similarly, a relatively dry 2016 water year marked by baseflow dominant streamflow discharge diluted relative sub-surface chloride concentrations, thus resulting in a lower BCI.

The monthly variability of tributary chloride loading and discharge separated by flow-path is shown in Fig. 7. Baseflow and runoff loading trends followed similar monthly patterns throughout the year. The highest median monthly loads attributed to baseflow and runoff occurred during March and April, where baseflow and runoff chloride loading accounted for approximately 22% and 6% of the total mean annual load, respectively. The lowest median monthly loads occurred in August and September, when baseflow and runoff loading accounted for 4% and 0.8% of the total mean annual load, respectively. Normalized monthly discharge, as denoted by the filled circles (Fig. 7), followed similar patterns to chloride loading and covered a slightly wider range in normalized median monthly flow (range: 0.23% to 12.6%) compared to normalized median monthly load (range: 0.35% to 11.6%).

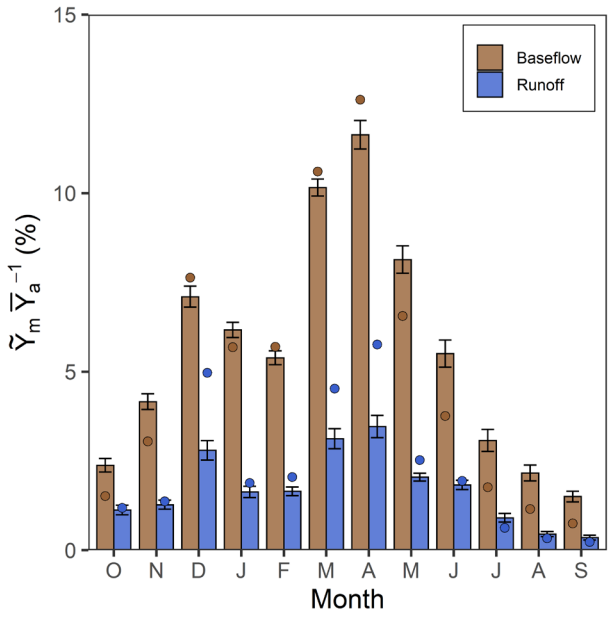

Fig. 7. Median monthly load (bars) and discharge (circles) as percent of mean annual load/discharge from October (O) through September (S). Data are averaged over all tributaries from 2000 through 2019.

The seasonal variation in tributary chloride export is dominated by inter-annual hydrologic variability. The high chloride loads during the spring (March – May) are attributed to the increased tributary discharge from snow-melt. Relatively lower loading in January and February

(compared to December and March) is attributed to snow-mass that has yet to melt. During the summer to early fall months (July – September), chloride loading from runoff (ranging from ~ 0.35% – 0.9% on average) slightly exceeds the chloride loading attributed to wet deposition, which accounts for approximately 0.11% of the mean annual chloride load for all tributaries. This suggests that trace amounts of residual road salts from the preceding winter application may be continually flushed from the watershed year-round.

3.2. Mass balance

The chloride mass input estimates from road salting practices are summarized in Fig. 8 and represent an average for the 20-year period of study. The minor tributary designation (MT) includes the French, Malagasco, Malden, Muddy, Trout, and West Boylston brooks. Total study period average annual chloride inputs from road salting practices were approximately 12,400 ton/year. However, yearly road salt application rates reported by the MassDOT were highly variable and are primarily governed by winter severity (MassDOT, 2017). Road salt application in the Quinapoxet River (QR) sub-basin alone accounted for 36% of that total. On average, road salt contributions from the MassDOT (82 lane-mi), city/town (498 lane-mi), and private maintenance (182 lane-mi) applications were 17%, 55%, and 28%, respectively. It was estimated that total road salt application in the 5.2 km^2 Gates Brook (GB) sub-basin exceeded that of the 78.5 km^2 Stillwater River (SR) sub-basin, a reflection of the stark differences in urbanization between the two catchments.

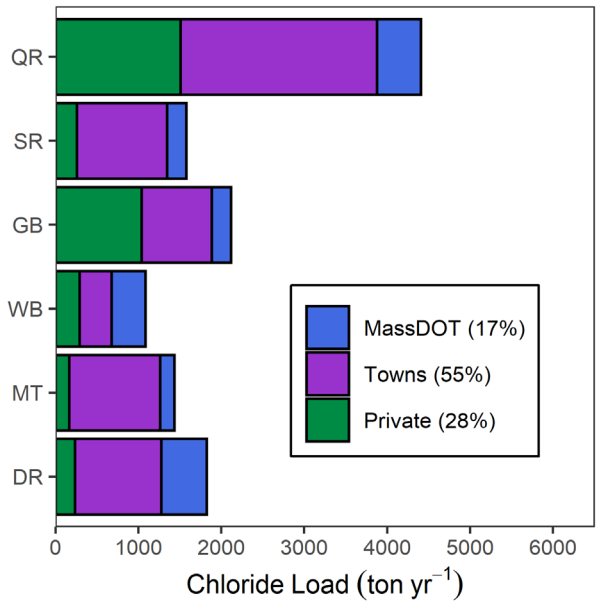

Fig. 8. Average annual chloride application from road salting practices by catchment and jurisdiction.

Results for the reservoir system chloride mass balance are provided in Fig. 9. Total tributary chloride export for the Quinapoxet River, Stillwater River, and Gates Brook were estimated from USGS gauges when data were available. Estimates for the direct runoff (DR) were derived from a flow-weighted average of chloride concentration in the adjacent minor tributaries. The remaining tributary contributions reflect LOADEST model output (excluding the linearly interpolated loading estimates for Trout Brook) and are combined into the MT designation with the exception of the standalone Waushacum Brook (WB). Additional imported chloride loads via the Quabbin Transfer (QT) are accounted for and contribute approximately 20% of the total reservoir chloride input, resulting from the QT providing ~ 50% of the annual average inflow at very low chloride concentrations (~ 7 mg/L). The final Quinapoxet River load was multiplied by the ratio of the total Quinapoxet River sub-basin area to its gauged area (equivalent to an increase of 8.7%) to account for additional mass input downstream of the monitoring station. Chloride inputs from septic effluent prior to 1997 were 600 ton/year, yet decreased to 240 ton/year in 1998 and further declined to approximately 50 ton/year in 2019 as the surrounding

towns gradually introduced wastewater collection through sanitary sewer systems. Chloride loads from wet deposition were 0.373 tons per km^2 per year, approximately 100 ton/year for the entire watershed. The average input from road salts and annual reservoir chloride export, via the Cosgrove Intake withdrawal and downstream releases to the Nashua River, reflect the chloride inputs and outputs to the entire reservoir system control volume. Water years are used to ensure that the winter salting season is not split into two calendar years.

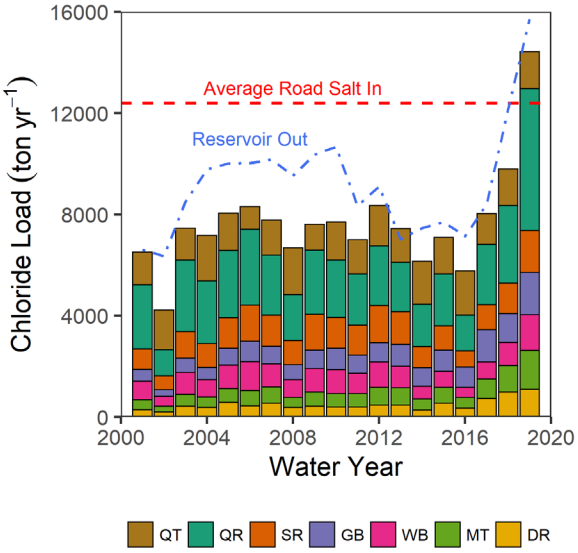

Fig. 9. Yearly chloride loading by reservoir input for water years 2001 through 2019.

While the year to year fluctuations in load and concentration are generally governed by hydrologic variability (Fig. 5), the increasing tributary loads beginning in water year 2017 seem to reflect the pervasive in-stream chloride trends observed throughout the watershed (Table 1). The 2019 water year marked the first instance when total tributary exports (13,000 ton/year) exceeded the mean road salt input (12,400 ton/year). The 2019 water year also marked a point in which the highest flow water year during the study period did not translate to a significant decrease in chloride concentration (4^{th} highest during the study period). A temporal lag between watershed inputs and reservoir withdrawals exists and can be partially attributed to the reservoir

mean hydraulic retention time of approximately 8 months. However, transport of constituent inputs from the west end of the reservoir to the Cosgrove Intake can occur in 2 to 15 days (Jeznach et al., 2016), depending on reservoir stratification and other factors. The differences between the reservoir withdrawal and watershed chloride loads may be attributed to current and legacy (prior to1998) septic exports (600 ton/year and 50 ton/year, respectively), unaccounted for chloride inputs from direct groundwater discharge into the reservoir, and model error.

The apparent decadal response of the Wachusett Reservoir and watershed to road salting are in agreement with Kelly et al. (2007), Novotny et al. (2009), and Shaw et al. (2012). Yearly road salt application rates were not available for city/town maintained roadways. However, MassDOT reduced application rates from 47 ton/lane-mi (2001-2010 average) to 35.7 ton/lane-mi (2011-2017 average) which may be attributed to the department's efforts to reduce road salt usage. Future tributary exports, and ultimately reservoir outputs, will be driven towards steady state conditions balanced by road salt inputs. If paved surface coverage remains stagnant, tributary chloride exports are expected to rise slightly in the near-term as they begin to approach a steady state with heavy road salting prior to 2010, before reaching new steady state conditions representative of reduced road salting efforts from the past decade. However, any further reduction in road salt application is not likely to be detected in reservoir outflow for at least several more years to decades and is certainly not expected to decrease the withdrawal CSMR below the proposed threshold of 0.5.

Individual chloride mass balances by sub-basin are plotted in Fig. 10. The long-term average annual chloride mass input via road salts (12,400 ton/year) and tributary export (6,200 ton/year) establishes an annual average chloride retention of 50% as sub-surface storage (Fig. 10a), in agreement with Howard and Haynes (1993), Meriano et al. (2009), and Perera et al. (2013).

Catchment export rates are ultimately governed by the time period for which the mass balance was performed and should asymptotically approach a steady state value of 1. The Quinapoxet River, Stillwater River, Gates Brook, and Waushacum Brook account for approximately 30%, 15%, 10%, and 10%, respectively, of the total chloride mass delivered to the Wachusett Reservoir. Collectively, these four tributaries constitute ~ 85% of the chloride load originating from the watershed.

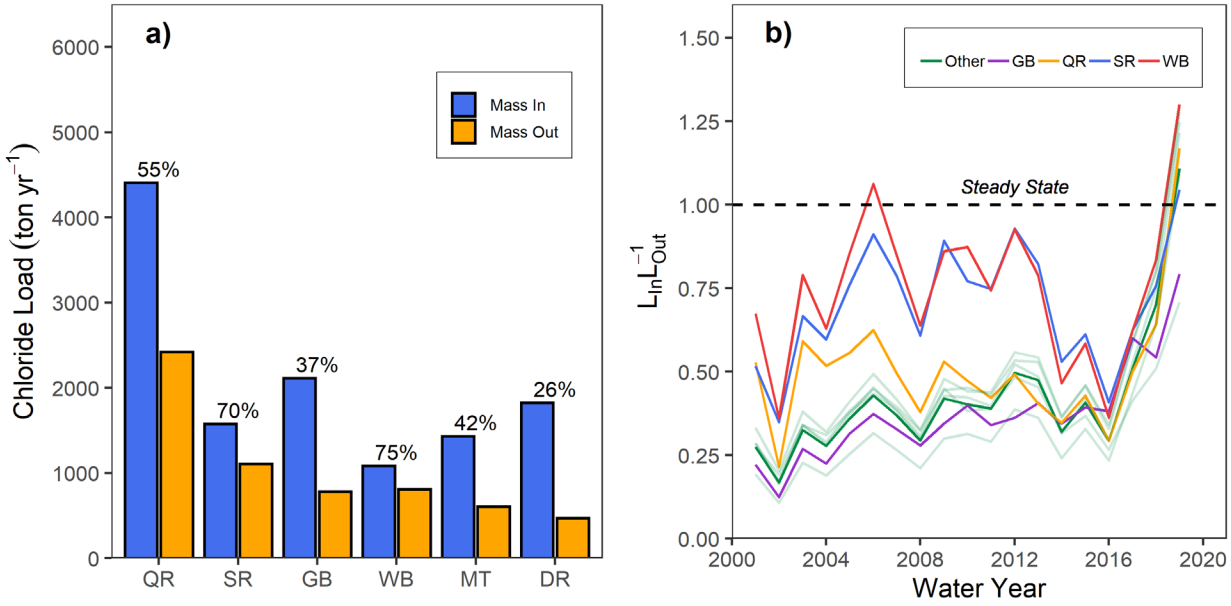

Fig. 10. Average (a) and timeseries (b) sub-basin chloride mass balances. 'Other' designation indicates average of minor tributaries and direct runoff (light green line).

Average catchment export ratios are used as a surrogate for sub-basin response rates (i.e. elapsed time between a surface pollutant loading event and corresponding tributary response via baseflow), with average rates closer to one indicating quicker catchment response. On average, the Quinapoxet River, Stillwater River, and Waushacum Brook catchments were marked by chloride export ratios inversely proportional to their respective catchment areas. The remaining sub-basins (typically less than 10 km^2) tended to export chloride at a rate much lower (<50%) than what was observed for the larger catchments. Even small urban sub-basins, such as the West

Boylston Brook, demonstrated export ratios suggestive of decadal response rates that are far greater than findings from prior research (Ostendorf, 2013). The uncertainty in road salt application estimation is likely exacerbated at the smaller scale where accurate and appropriate lane-mile quantification and attribution becomes crucial. Furthermore, the relatively quick response rates in the Quinapoxet River, Stillwater River, and Waushacum Brook may be exaggerated by strikingly low city/town application rates reported by the towns of Holden (14.6 ton NaCl/lane-mi per year) and Sterling (12.6 ton NaCl/lane-mi per year) that were far lower than the city/town average of 31.6 ton NaCl/lane-mi per year.

3.3.1. LOADEST model performance

LOADEST model cumulative distribution functions (CDFs) for the four largest chloride exporters in the watershed (Fig. 11) and comprehensive model statistics (Table 5) indicate good, yet varied, performance for both flow-path models. Total chloride loading model R^2 and NSE values ranged from 0.74 – 0.92 and 0.56 – 0.84, respectively. Baseflow load regressions shared similar R^2 and NSE statistics to their total load counterparts, ranging from 0.70 – 0.92 and 0.44 – 0.88, respectively. The observed data distribution is well fit to the simulated CDF and within the 95% confidence interval distribution. The high serial correlation of residuals (>0.3) observed for all models were not considered detrimental due to the universally low load bias percentages (< 5%). The Trout Brook LOADEST estimates are ignored in this study due to poor model performance (NSE < 0.5) that was attributed to a lack of data.

Table 5. LOADEST model coefficient of determination (R^2), Nash-Sutcliffe Efficiency (NSE), bias percentage (Bp), and serial correlation of residuals (SCORR) by tributary and flow-path.

Tributary	Total				Baseflow			
	R^2	NSE	Bp	SCORR	R^2	NSE	Bp	SCORR
GB	0.92	0.84	-0.50	0.41	0.93	0.84	-0.82	0.54
QR	0.88	0.66	-2.05	0.51	0.87	0.78	-0.75	0.51
SR	0.74	0.56	-0.39	0.49	0.75	0.49	0.12	0.41
FB	0.77	0.69	-0.09	0.58	0.74	0.79	0.70	0.61
MgB	0.80	0.68	-0.25	0.59	0.78	0.68	0.23	0.55
MaB	0.92	0.82	-0.47	0.50	0.91	0.86	-0.15	0.46
MuB	0.91	0.75	-1.59	0.44	0.89	0.86	-0.66	0.53
WB	0.92	0.84	1.87	0.56	0.93	0.90	1.97	0.55
WBB	0.89	0.75	-0.81	0.34	0.85	0.76	-0.29	0.30
TB[1]	0.68	0.30	-3.94	0.40	0.75	0.41	-3.71	0.45

[1] Excluded in analysis due to poor fit

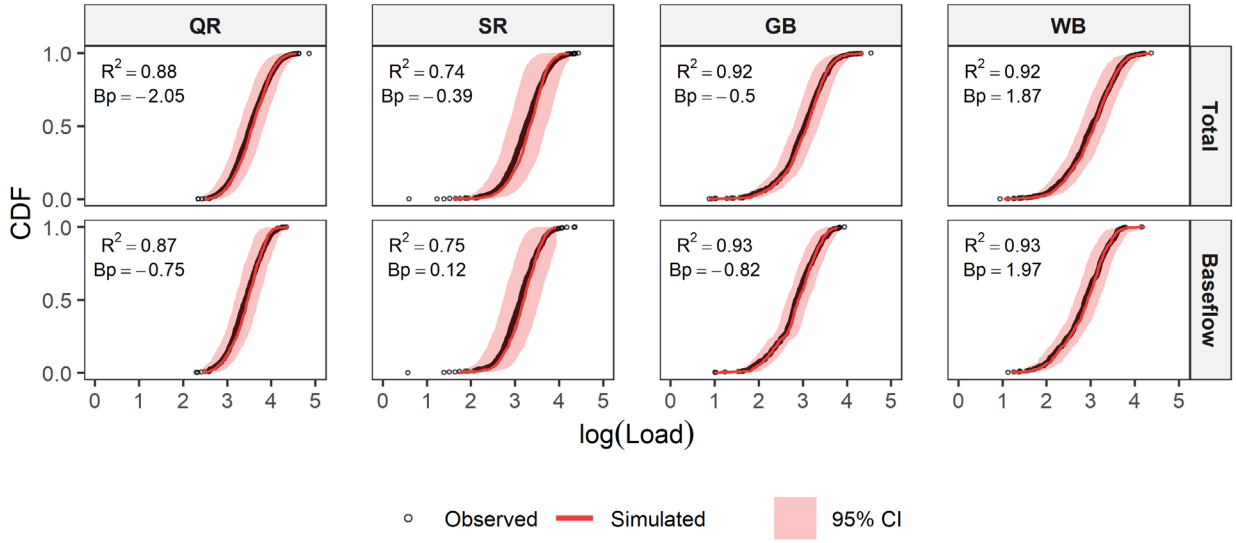

Fig. 11. LOADEST model cumulative distribution functions (CDFs) with coefficient of determination (R^2) and bias percentage (Bp) for the Quinapoxet River (QR), Stillwater River (SR), Gates Brook (GB), and Waushacum Brook (WB).

3.3.2. Comparison to high-frequency data

The presence of USGS continuously (~daily) monitored SC at the Quinapoxet River, Stillwater River, and Gates Brook sites allowed for an evaluation of the regression methods employed. Monthly and yearly load errors, expressed as the normalized root mean square error (Eq. 4), between the models (LOADEST) and linear interpolations between the regression model

calibration datasets (Int.) were compared to known (USGS) loads (Table 6). In several instances, daily measurements by the USGS were not available. Therefore, months that had five or more missing daily measurements were removed from error calculations. Years that did not have a full 12 months of data were also removed.

$$NRMSE = \sqrt{\frac{\sum_{i=1}^{n}(\hat{y}_i - y_i)^2}{n}}\,\bar{y}_i^{-1} \quad \text{(Eq. 4)}$$

Where $\hat{y}_i$ are simulated results, y_i are observed, and $\bar{y}_i$ is the mean of observed data.

Table 6. Monthly and yearly NRMSE between observed USGS loading and load estimation methods.

Trib.	Monthly			Yearly		
	Int.	*LOADEST*	*Samples*	*Int.*	*LOADEST*	*Samples*
QR	0.41	0.32	227	0.17	0.19	13
SR	0.78	0.68	227	0.49	0.40	13
GB[1]	0.26	0.22	74	0.06	0.07	3

[1] Period of record: 2012-05-09 through 2019

Load estimation with LOADEST consistently offered a closer fit to USGS observations in comparison to that from the linear interpolation. LOADEST and interpolation methods yielded similar results at the yearly timestep, with the exception of the Stillwater River where LOADEST outperformed the interpolation. The reduced load estimation accuracy for both methods at smaller (monthly) timesteps is noted in Pellerin et al. (2014) and most likely a result of under-represented extreme loading events that are often absent from field-measurements. The high LOADEST errors (NRMSE range from 0.40 to 0.78) from the Stillwater River model may be a result of an intermittent series of significant loading events from 2001 through 2008 observed in the DCR data that weren't reciprocated in the USGS data. Thus, the Stillwater River regression model is partially undermined by calibrating to a potentially erroneous subset of concentration data. Errors in load estimation may also have been influenced by inconsistent SC

measurements between the USGS and DCR, although this is not expected to have a significant impact on monthly or yearly load estimates.

3.3.3. Sensitivity to baseflow separation

The sensitivity of results to variants of four popular hydrograph separation methods are shown in Fig. 12. Mean BLIs using the HYSEP-F (0.76), HYSEP-S (0.76), PART (0.75), and Eckhardt (0.75) methods were nearly identical and corresponded to BCIs ranging from 1.07 to 1.1. The L&H methods produced a wide range of BLI (0.76 to 0.55) and BCI (1.13 to 1.22) results. The L&H-2 and L&H-3 techniques also produced the highest variability in BLI and BCI estimates among the tributaries and water years for which the results are averaged over. Ultimately, the mean tributary BLI (0.74) and BCI (1.12) for all separation scenarios is in close agreement with study results ($\overline{BLI}$ = 0.74; $\overline{BCI}$ = 1.13) using the HYSEP-L method.

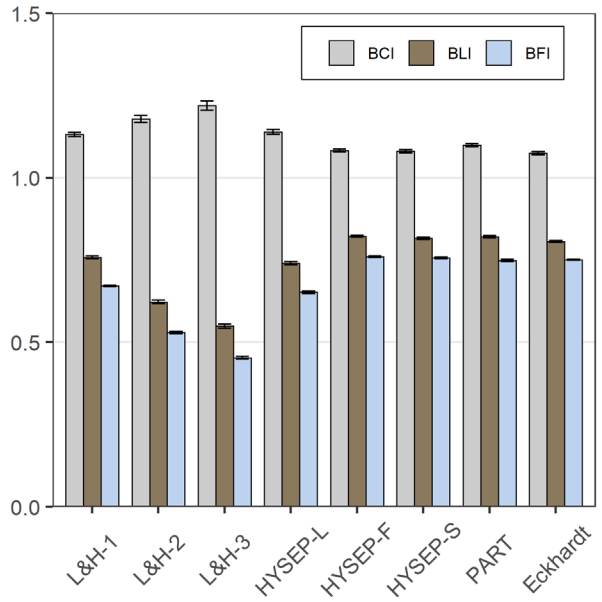

Fig. 12. Baseflow chloride index, baseflow load index, and baseflow index sensitivities to eight hydrograph separation methodologies. Individual bar plots reflect average metric values by water year (2001-2019) for all modeled tributaries (9) with standard error bars.

Baseflow dominated chloride loading and transport within the reservoir watershed holds true for this sensitivity analysis. A significant range of BFIs result from the eight different hydrograph separation methods, as noted in Eckhardt (2008) and Partington et al. (2012), with baseflow indices generally positively correlated with BLI and negatively correlated with BCI. However, chloride loading and transport through baseflow remains the prevailing condition, as demonstrated by BLIs greater than 0.5 and BCIs greater than 1. The variability in BCI also tended to increase with lower values of BFI and is attributed to the sensitivity in BCI subject to lower magnitudes of BLI and BFI.

4. Conclusion

Chloride loading into the Wachusett Reservoir is dominated by inputs from road salting practices. Statistically based load estimation methods reveal that road salts are preferentially transported into the sub-surface, with approximately 74% of the tributary chloride export delivered via baseflow. Since 2000, chloride mass balances reveal that the 2019 water year marked the first instance when watershed export reached a level similar to the road salt input. The rural nature of the watershed and predominantly low impervious surface coverage acts to delay chloride mass transport from initial application to reservoir inflow.

This study notes the relationship between water corrosivity and chloride, mainly via the CSMR metric. Greater Boston water supply management authorities concerned with lead corrosion should recognize that (1) chloride concentrations in the Wachusett Reservoir and tributaries are not expected to increase significantly beyond current levels so long as paved surface coverage remains unchanged and (2) any reductions in road salt application are not likely to be reflected in surface water quality for several years to decades. The current chloride and

sulfate levels in the reservoir should therefore be factored in to corrosion control decision-making processes.

References

Ahlfeld, D., A. Joaquin, J. Tobiason, and D. Mas (2003), Case study: Impact of reservoir stratification on interflow travel time, J. Hydraul. Eng., 129(12), 966-975.

Bubeck, R. C. and R. S. Burton (1989), Changes in chloride concentrations, mixing patterns, and stratification characteristics of Irondequoit Bay, Monroe County, New York, after decreased use of road-deicing salts, 1974-1984, vol. 87, , Department of the Interior, US Geological Survey, .

Chen, D., M. Hu, Y. Guo, and R. A. Dahlgren (2015), Reconstructing historical changes in phosphorus inputs to rivers from point and nonpoint sources in a rapidly developing watershed in eastern China, 1980–2010, Sci. Total Environ., 533, 196-204.

Cohn, T. A., D. L. Caulder, E. J. Gilroy, L. D. Zynjuk, and R. M. Summers (1992), The validity of a simple statistical model for estimating fluvial constituent loads: an empirical study involving nutrient loads entering Chesapeake Bay, Water Resour. Res., 28(9), 2353-2363.

Cohn, T. A., L. L. Delong, E. J. Gilroy, R. M. Hirsch, and D. K. Wells (1989), Estimating constituent loads, Water Resour. Res., 25(5), 937-942.

Collins, S. J. and R. W. Russell (2009), Toxicity of road salt to Nova Scotia amphibians, Environmental Pollution, 157(1), 320-324.

Dailey, K. R., K. A. Welch, and W. B. Lyons (2014), Evaluating the influence of road salt on water quality of Ohio rivers over time, Appl. Geochem., 47, 25-35.

Dierauer, J. and P. Whitfield (2017), Package 'FlowScreen', The Comprehensive R Archive Network (CRAN).

Duan, W., K. Takara, B. He, P. Luo, D. Nover, and Y. Yamashiki (2013), Spatial and temporal trends in estimates of nutrient and suspended sediment loads in the Ishikari River, Japan, 1985 to 2010, Sci. Total Environ., 461, 499-508, doi:10.1016/j.scitotenv.2013.05.022.

Eckhardt, K. (2008), A comparison of baseflow indices, which were calculated with seven different baseflow separation methods, Journal of Hydrology, 352(1-2), 168-173.

Eckhardt, K. (2005), How to construct recursive digital filters for baseflow separation, Hydrological Processes: An International Journal, 19(2), 507-515.

Edwards, M. and S. Triantafyllidou (2007), Chloride-to-sulfate mass ratio and lead leaching to water, Journal-American Water Works Association, 99(7), 96-109.

Fuka, D. R., M. T. Walter, J. A. Archibald, T. S. Steenhuis, Z. M. Easton, M. D. Fuka, and T. KeepSource (2014), Package 'EcoHydRology',.

Godwin, K. S., S. D. Hafner, and M. F. Buff (2003), Long-term trends in sodium and chloride in the Mohawk River, New York: the effect of fifty years of road-salt application, Environmental pollution, 124(2), 273-281.

Hagemann, M. and M. Park (2014), Trends in tributary water quality in a water supply reservoir, Journal-American Water Works Association, 106(4), E212-E224.

He, S., Y. Hao, J. Wu, and J. Lu (2020), Estimation of baseflow nitrate loads by a recursive tracing source algorithm in a rainy agricultural watershed, Hydrol. Process., 34(2), 441-454, doi:10.1002/hyp.13597.

Hintz, W. D., B. M. Mattes, M. S. Schuler, D. K. Jones, A. B. Stoler, L. Lind, and R. A. Relyea (2017), Salinization triggers a trophic cascade in experimental freshwater communities with varying food-chain length, Ecol. Appl., 27(3), 833-844.

Hodgkins, G. A. and R. W. Dudley (2011), Historical summer base flow and stormflow trends for New England rivers, Water Resour. Res., 47(7).

Howard, K. W. and J. Haynes (1993), Groundwater contamination due to road de-icing chemicals—salt balance implications, Geosci. Can., 20(1).

Huling, E. E. and T. C. Hollocher (1972), Groundwater contamination by road salt: Steady-state concentrations in East Central Massachusetts, Science, 176(4032), 288-290.

Hutchinson, F. E. and B. E. Olson (1967), THE RELATIONSHIP OF ROAD SALT APPLICATIONS TO SODIUM AND CHLORIDE ION LEVELS IN SOIL BORDERING MAJOR HIGHWAYS, Highway Research Record(193).

Jeznach, L. C., C. Jones, T. Matthews, J. E. Tobiason, and D. P. Ahlfeld (2016), A framework for modeling contaminant impacts on reservoir water quality, Journal of Hydrology, 537, 322-333, doi:https://doi.org/10.1016/j.jhydrol.2016.03.041.

Jha, M. K., P. W. Gassman, and J. G. Arnold (2007), Water quality modeling for the Raccoon River watershed using SWAT, Trans. ASABE, 50(2), 479-493.

Judd, J. H. (1970), Lake stratification caused by runoff from street deicing, Water Res., 4(8), 521-532.

Judd, K. E., H. E. Adams, N. S. Bosch, J. M. Kostrzewski, C. E. Scott, B. M. Schultz, D. H. Wang, and G. W. Kling (2005), A case history: effects of mixing regime on nutrient dynamics and community structure in Third Sister Lake, Michigan during late winter and early spring 2003, Lake Reserv. Manage., 21(3), 316-329.

Karalekas Jr, P. C., C. R. Ryan, and F. B. Taylor (1983), Control of lead, copper, and iron pipe corrosion in Boston, Journal-American Water Works Association, 75(2), 92-95.

Karraker, N. E., J. P. Gibbs, and J. R. Vonesh (2008), Impacts of road deicing salt on the demography of vernal pool-breeding amphibians, Ecol. Appl., 18(3), 724-734.

Kelly, T. D., G. R. Matos, D. A. Buckingham, C. A. DiFrancesco, K. E. Porter, and C. Berry (2010), Historical statistics for mineral and material commodities in the United States, US Geological Survey data series, 140, 1.

Kelly, V. R., G. M. Lovett, K. C. Weathers, S. E. Findlay, D. L. Strayer, D. J. Burns, and G. E. Likens (2007), Long-term sodium chloride retention in a rural watershed: legacy effects of road salt on streamwater concentration, Environ. Sci. Technol., 42(2), 410-415.

Koretsky, C. M., A. MacLeod, R. J. Sibert, and C. Snyder (2012), Redox stratification and salinization of three kettle lakes in southwest Michigan, USA, Water, Air, & Soil Pollution, 223(3), 1415-1427.

Likens, G. E. and D. C. Buso (2010), Salinization of Mirror Lake by road salt, Water Air Soil Pollut., 205(1-4), 205.

Lyne, V. and M. Hollick (1979), Stochastic time-variable rainfall-runoff modelling, paper presented at Institute of Engineers Australia National Conference, Institute of Engineers Australia Barton, Australia.

Lytle, D. A., P. Sarin, and V. L. Snoeyink (2005), The effect of chloride and orthophosphate on the release of iron from a cast iron pipe section, Journal of Water Supply: Research and Technology-AQUA, 54(5), 267-281.

MassDOT (2017), MassDOT Snow and Ice Control Program: 2017 Environmental Status and Planning Report, in .

Masten, S. J., S. H. Davies, and S. P. Mcelmurry (2016), Flint water crisis: what happened and why? Journal-American Water Works Association, 108(12), 22-34.

Meriano, M., N. Eyles, and K. W. F. Howard (2009), Hydrogeological impacts of road salt from Canada's busiest highway on a Lake Ontario watershed (Frenchman's Bay) and lagoon, City of Pickering, Journal of Contaminant Hydrology, 107(1), 66-81, doi:https://doi.org/10.1016/j.jconhyd.2009.04.002.

Moore, J., R. M. Fanelli, and A. J. Sekellick (2019), High-frequency data reveal deicing salts drive elevated specific conductance and chloride along with pervasive and frequent exceedances of the US Environmental Protection Agency aquatic life criteria for chloride in urban streams, Environ. Sci. Technol., 54(2), 778-789.

Nash, J. E. and J. V. Sutcliffe (1970), River flow forecasting through conceptual models part Iâ€”A discussion of principles, Journal of hydrology, 10(3), 282-290.

Nathan, R. J. and T. A. McMahon (1990), Evaluation of automated techniques for base flow and recession analyses, Water Resour. Res., 26(7), 1465-1473.

Ng, D. and Y. Lin (2016), Effects of pH value, chloride and sulfate concentrations on galvanic corrosion between lead and copper in drinking water, Environ.Chem, 13(4), 602-610.

Nguyen, C. K., B. N. Clark, K. R. Stone, and M. A. Edwards (2011), Role of chloride, sulfate, and alkalinity on galvanic lead corrosion, Corrosion, 67(6), 065005-9.

Nimiroski, M. T. and M. C. Waldron (2002), Sources of sodium and chloride in the Scituate Reservoir drainage basin, Rhode Island, US Department of the Interior, US Geological Survey, .

Novotny, E. V., D. Murphy, and H. G. Stefan (2008), Increase of urban lake salinity by road deicing salt, Sci. Total Environ., 406(1-2), 131-144.

Novotny, E. V., A. R. Sander, O. Mohseni, and H. G. Stefan (2009), Chloride ion transport and mass balance in a metropolitan area using road salt, Water Resour. Res., 45(12).

Novotny, E. V. and H. G. Stefan (2012), Road salt impact on lake stratification and water quality, J. Hydraul. Eng., 138(12), 1069-1080.

Ostendorf, D. W. (2013), Hydrograph and chloride pollutograph analysis of Hobbs Brook reservoir subbasin in eastern Massachusetts, journal of Hydrology, 503, 123-134.

Ostendorf, D. W. and C. J. Kilbridge (2011), Impact case study year II: aquitard hydraulics and aquifer transport in the White Lodge wellfield of the Dedham-Westwood water district, Journal of the New England Water Works Association, 125(3), 229.

Panno, S. V., K. C. Hackley, H. H. Hwang, S. E. Greenberg, I. G. Krapac, S. Landsberger, and D. J. O'kelly (2006), Characterization and identification of Na-Cl sources in ground water, Groundwater, 44(2), 176-187.

Partington, D., P. Brunner, C. T. Simmons, A. D. Werner, R. Therrien, H. R. Maier, and G. C. Dandy (2012), Evaluation of outputs from automated baseflow separation methods against simulated baseflow from a physically based, surface water-groundwater flow model, Journal of Hydrology, 458, 28-39.

Pellerin, B. A., B. A. Bergamaschi, R. J. Gilliom, C. G. Crawford, J. Saraceno, C. P. Frederick, B. D. Downing, and J. C. Murphy (2014), Mississippi River nitrate loads from high frequency sensor measurements and regression-based load estimation, Environ. Sci. Technol., 48(21), 12612-12619.

Perera, N., B. Gharabaghi, and K. Howard (2013), Groundwater chloride response in the Highland Creek watershed due to road salt application: A re-assessment after 20 years, Journal of Hydrology, 479, 159-168.

Pettyjohn, W. A. and R. J. Henning (1979), Preliminary estimate of regional effective ground-water recharge rates in Ohio, Ohio State University. Water Resources Center, .

Pieper, K. J., R. Martin, M. Tang, L. Walters, J. Parks, S. Roy, C. Devine, and M. A. Edwards (2018), Evaluating water lead levels during the Flint water crisis, Environ. Sci. Technol., 52(15), 8124-8132.

Pieper, K. J., M. Tang, and M. A. Edwards (2017), Flint water crisis caused by interrupted corrosion control: investigating "ground zero" home, Environ. Sci. Technol., 51(4), 2007-2014.

Ramakrishna, D. M. and T. Viraraghavan (2005), Environmental impact of chemical deicers–a review, Water Air Soil Pollut., 166(1-4), 49-63.

Richburg, J. A., W. A. Patterson, and F. Lowenstein (2001), Effects of road salt and Phragmites australis invasion on the vegetation of a western Massachusetts calcareous lake-basin fen, Wetlands, 21(2), 247-255.

Runkel, R. L., C. G. Crawford, and T. A. Cohn (2004), Load Estimator (LOADEST): A FORTRAN Program for Estimating Constituent Loads in Streams and Rivers, Load Estimator (LOADEST): A FORTRAN program for estimating constituent loads in streams and rivers.

Rutledge, A. T. (1998), Computer programs for describing the recession of ground-water discharge and for estimating mean ground-water recharge and discharge from streamflow records: Update, US Department of the Interior, US Geological Survey, .

Sanford, W. E. and J. P. Pope (2013), Quantifying groundwater's role in delaying improvements to Chesapeake Bay water quality, Environ. Sci. Technol., 47(23), 13330-13338.

Schilling, K. and Y. Zhang (2004), Baseflow contribution to nitrate-nitrogen export from a large, agricultural watershed, USA, Journal of Hydrology, 295(1-4), 305-316.

Shaw, S. B., R. D. Marjerison, D. R. Bouldin, Parlange Jean-Yves, and W. M. Todd (2012), Simple Model of Changes in Stream Chloride Levels Attributable to Road Salt Applications, J. Environ. Eng., 138(1), 112-118, doi:10.1061/(ASCE)EE.1943-7870.0000458.

Shope, C. L. and C. E. Angeroth (2015), Calculating salt loads to Great Salt Lake and the associated uncertainties for water year 2013; updating a 48 year old standard, Sci. Total Environ., 536, 391-405.

Sibert, R. J., C. M. Koretsky, and D. A. Wyman (2015), Cultural meromixis: Effects of road salt on the chemical stratification of an urban kettle lake, Chem. Geol., 395, 126-137.

Sloto, R. A. and M. Y. Crouse (1996), HYSEP: A computer program for streamflow hydrograph separation and analysis, Water-resources investigations report, 96, 4040.

Spongberg, M. E. (2000), Spectral analysis of base flow separation with digital filters, Water Resour. Res., 36(3), 745-752.

Starn, J. J. and K. Belitz (2018), Regionalization of groundwater residence time using metamodeling, Water Resour. Res., 54(9), 6357-6373.

Stets, E. G., C. J. Lee, D. A. Lytle, and M. R. Schock (2018), Increasing chloride in rivers of the conterminous US and linkages to potential corrosivity and lead action level exceedances in drinking water, Sci. Total Environ., 613, 1498-1509.

Tobiason, J. E., D. P. Ahlfeld, A. Joaquin, and D. Mas (2002), Water quality in MDC reservoirs, Project 1: Wachusett Reservoir water quality modeling, Rep.Submitted to Metropolitan District Commission, Division of Watershed Management, Boylston, Mass.

Trowbridge, P. R., J. S. Kahl, D. A. Sassan, D. L. Heath, and E. M. Walsh (2010), Relating road salt to exceedances of the water quality standard for chloride in New Hampshire streams, Environ. Sci. Technol., 44(13), 4903-4909.

Vitale, S. A., G. A. Robbins, and L. A. McNaboe (2017), Impacts of road salting on water quality in fractured crystalline bedrock, J. Environ. Qual., 46(2), 288-294.

Wang, Y., X. Liu, Y. Li, F. Liu, J. Shen, Y. Li, Q. Ma, J. Yin, and J. Wu (2015), Rice agriculture increases base flow contribution to catchment nitrate loading in subtropical central China, Agriculture, Ecosystems & Environment, 214, 86-95, doi:https://doi.org/10.1016/j.agee.2015.08.017.

Wilcox, D. A. (1986), The effects of deicing salts on vegetation in Pinhook Bog, Indiana, Canadian Journal of Botany, 64(4), 865-874.

Wyman, D. A. and C. M. Koretsky (2018), Effects of road salt deicers on an urban groundwater-fed kettle lake, Appl. Geochem., 89, 265-272.

Zhu, Y., L. Chen, G. Wei, S. Li, and Z. Shen (2019), Uncertainty assessment in baseflow nonpoint source pollution prediction: the impacts of hydrographic separation methods, data sources and baseflow period assumptions, Journal of Hydrology, 574, 915-925.